# Capturing molecular multimode relaxation processes in excitable gases based on decomposition of acoustic relaxation spectra

OPEN ACCESS
IOP Publishing
Measurement Science and Technology
Meas. Sci. Technol. **28** (2017) 085008 (9pp)
https://doi.org/10.1088/1361-6501/aa544d

# Capturing molecular multimode relaxation processes in excitable gases based on decomposition of acoustic relaxation spectra

**Ming Zhu[1], Tingting Liu[1], Shu Wang[1] and Kesheng Zhang[2]**

[1] School of Electronic Information and Communications, Huazhong University of Science and Technology, Wuhan 430074, People's Republic of China
[2] School of Information Engineering, Guizhou Institute of Technology, Guiyang 550003, People's Republic of China

E-mail: zhuming@mail.hust.edu.cn

Received 29 July 2016, revised 30 November 2016
Accepted for publication 16 December 2016
Published 17 July 2017

**Abstract**

Existing two-frequency reconstructive methods can only capture primary (single) molecular relaxation processes in excitable gases. In this paper, we present a reconstructive method based on the novel decomposition of frequency-dependent acoustic relaxation spectra to capture the entire molecular multimode relaxation process. This decomposition of acoustic relaxation spectra is developed from the frequency-dependent effective specific heat, indicating that a multi-relaxation process is the sum of the interior single-relaxation processes. Based on this decomposition, we can reconstruct the entire multi-relaxation process by capturing the relaxation times and relaxation strengths of $N$ interior single-relaxation processes, using the measurements of acoustic absorption and sound speed at $2N$ frequencies. Experimental data for the gas mixtures $CO_2$–$N_2$ and $CO_2$–$O_2$ validate our decomposition and reconstruction approach.

Keywords: measurement of molecular relaxation, multimode relaxation in gases, acoustic relaxation spectra, relaxation time, relaxation strength

(Some figures may appear in colour only in the online journal)

## 1. Introduction

In the past several decades, the study of molecular relaxation in gases has substantially promoted the development of many fields, such as anomalous absorption in polyatomic gases [1–4], molecular lasers [5, 6], thermal phonons [7], quantum computation [8–10], plasma discharges [11, 12] and so on. The frequency dependencies of acoustic absorption and sound speed both are determined by molecular relaxation in excitable gases [2, 3]. Moreover, air-coupled acoustic transducers, such as parking sensors, are cheap and robust [13] and thus acoustic measurement is a very promising, efficient and convenient tool for exciting, capturing and exploring relaxation in gases. In practice, however, it is quite difficult to measure the entire molecular relaxation process by changing the frequency of transducers over a sufficiently wide range, since commercially available transducers have fixed resonance frequencies [13, 14]. Since relaxation time varies inversely with gas pressure, the traditional approach is to make the measurements at a handful of frequencies while varying gas pressure over a wide range [15–20]. This provides a broad range of frequency–pressure ratios ($f/p$) to cover the entire relaxation process. However, the necessary pressures are often so small that the acoustic signals are swamped in noise or so large



 

that the non-ideality of the gas needs to be considered [21]. Furthermore, the requirement to make many measurements at different pressures is time consuming. Thus, it is desirable to develop an efficient acoustic approach to measure molecular relaxation in gases.

To address the drawbacks due to varying gas pressure, Petculescu and Lueptow (PL) presented a two-frequency reconstructive algorithm to synthesize primary (single) molecular relaxation processes at a single pressure [21]. However, the algorithm utilizes the frequency dependence of the effective specific heat of gases for the reconstruction, which requires the gas density to be measured with the necessary pre-processing of the gases. Unlike the effective specific heat approach, the acoustic relaxation spectra of gases can be obtained by only measuring acoustic absorption and sound speed, which avoids the complexity of detecting the gas density. Based on this fact, we recently proposed a method to capture the primary relaxation processes by reconstructing the acoustic relaxation spectra [22]. However, compared with the traditional measurements with varying gas pressure, these fast reconstructive algorithms cannot capture the entire molecular multimode relaxation process for systems having more than one dominant interior single-relaxation process, which results in the loss of significant relaxation information for various applications, such acoustic gas sensing [20, 23–26].

In this paper, we decompose the acoustic relaxation spectrum of a molecular multimode relaxation process into spectra of interior single-relaxation processes. Based on this decomposition, we can reconstruct entire multi-relaxation processes by capturing the relaxation times and relaxation strengths of $N$ interior single-relaxation processes using measurements at $2N$ operating frequencies. Experimental data validate our decomposition and reconstruction approach. The present paper is organized as follows. In section 2 we introduce the decomposition of the acoustic spectra of multimode relaxation processes. In section 3 we demonstrate the reconstruction of the entire molecular multi-relaxation process in gases. Section 4 concludes the paper.

## 2. Decomposition of acoustic relaxation spectra of gases

### 2.1. General expression of acoustic relaxation spectra

The molecular collisional relaxation processes resulting from acoustic propagation in excitable gases (diatomic or polyatomic gases and their mixtures) can be expressed as an effective acoustic wave number $\tilde{k}(\omega)$ which depends on the frequency-dependent phase speed $c(\omega)$ and the molecular relaxation absorption coefficient $\alpha_r(\omega)$ [21]:

$$\tilde{k}(\omega) = \frac{\omega}{c(\omega)} - \mathrm{i}\alpha_r(\omega), \tag{1}$$

where $\omega = 2\pi f$ is the acoustic angular frequency and $\mathrm{i} = \sqrt{-1}$.

The graphical representation of the relaxation processes is the acoustic relaxation spectra $\mu(\omega)$, which represent the frequency dependence of the dimensionless relaxation absorption coefficient $\alpha_r\lambda$, where $\lambda$ is the wavelength of sound. Thus $\mu(\omega)$ can be represented in terms of the real and imaginary parts of $\tilde{k}(\omega)$:

$$\mu(\omega) = \alpha_r(\omega)\frac{c(\omega)}{f} = -2\pi\frac{\mathrm{Im}(\tilde{k}(\omega))}{\mathrm{Re}(\tilde{k}(\omega))}. \tag{2}$$

$\tilde{k}(\omega)$ can also be expressed in terms of the frequency-dependent effective isochoric molar specific heat of gases $C_V^{\mathrm{eff}}(\omega)$ [21]:

$$\tilde{k}(\omega) = \omega\sqrt{\frac{\rho_0}{p_0}}\sqrt{\frac{C_V^{\mathrm{eff}}(\omega)}{C_V^{\mathrm{eff}}(\omega)+R}}, \tag{3}$$

where $\rho_0$ and $p_0$ are the equilibrium gas density and pressure, respectively, and $R = 8.31$ J mol$^{-1}$ K$^{-1}$ is the universal gas constant.

From equations (2) and (3), we can see that the effective specific heat determines the relaxation processes and the acoustic spectra of gases. Therefore, the acoustic relaxation spectra $\mu(\omega)$ can be expressed by using the effective specific heat $C_V^{\mathrm{eff}}(\omega)$. Similar to $\tilde{k}(\omega)$, $C_V^{\mathrm{eff}}(\omega)$ is also a complex number and can be written as $C_V^{\mathrm{eff}}(\omega) \equiv x(\omega) - \mathrm{i}y(\omega)$. Thus, we combine (1) with (3) to obtain

$$\tilde{k}(\omega) = \frac{\omega}{c(\omega)} - \mathrm{i}\alpha_r(\omega) = \omega\sqrt{\frac{\rho_0}{P_0}}\sqrt{\frac{x(\omega)-\mathrm{i}y(\omega)}{x(\omega)-\mathrm{i}y(\omega)+R}}. \tag{4}$$

To find the dependence of $\mu(\omega)$ upon $x(\omega)$ and $y(\omega)$, we square equation (4) for $(\tilde{k}(\omega))^2$ and expand two items on the right of the square of equation (4) respectively as

$$\left(\frac{\omega}{c(\omega)}\right)^2 - 2\mathrm{i}\frac{\omega}{c(\omega)}\alpha_r(\omega) - (\alpha_r(\omega))^2 = \omega^2\frac{\rho_0}{P_0}\frac{x^2(\omega)+Rx(\omega)+y^2(\omega)-\mathrm{i}Ry(\omega)}{(x(\omega)+R)^2+y^2(\omega)}. \tag{5}$$

Since acoustic relaxation spectra are bell-shaped curves with a maximum $\mu_{\max}$ [2–4], we have $\alpha_r(\omega) \leqslant \frac{\mu_{\max}}{2\pi}\frac{\omega}{c(\omega)}$ from equation (2). Also, because $\frac{\mu_{\max}}{2\pi} < 10^{-1}$ for most gases and their mixtures at room temperature [15–20] (e.g. the values are less than 0.02 for $CO_2$ and 0.0001 for $N_2$ respectively), we have $(\alpha_r(\omega))^2 \ll \left(\frac{\omega}{c(\omega)}\right)^2$. So we can ignore the term $(\alpha_r(\omega))^2$ for the left side of equation (5). Then the acoustic relaxation spectra $\mu(\omega)$ can also be calculated by the real and imaginary parts of $(\tilde{k}(\omega))^2$:

$$\mu(\omega) = \pi\frac{2\frac{\omega}{c(\omega)}\alpha_r(\omega)}{\left(\frac{\omega}{c(\omega)}\right)^2} = -\pi\frac{\mathrm{Im}\,[(\tilde{k}(\omega))^2]}{\mathrm{Re}\,[(\tilde{k}(\omega))^2]}. \tag{6}$$

Combining (5) with (6), the general expression for acoustic relaxation spectra using the real and imaginary parts of effective specific heat can be obtained as

$$\mu(\omega) = A_\mu y(\omega),\ A_\mu = \frac{\pi R}{x^2(\omega)+Rx(\omega)+y^2(\omega)}. \tag{7}$$

**Table 1.** The normal vibrational frequencies $\upsilon$ and the corresponding vibrational specific heats $C_{\mathrm{V}}^{\mathrm{vib}}$ for some gases at $T = 300\,\mathrm{K}$.

| Gas | $\upsilon/(\mathrm{cm}^{-1})$ | $C_{\mathrm{V}}^{\mathrm{vib}}/\mathrm{J\ mol^{-1}\ K^{-1}}$ |
|---|---|---|
| $N_2$ [19] | $\upsilon = 2331$ | $1.38 \times 10^{-2}$ |
| $O_2$ [19] | $\upsilon = 1554$ | $2.67 \times 10^{-1}$ |
| $Cl_2$ [3] | $\upsilon = 577$ | 4.55 |
| $CH_4$ [19] | $\upsilon_1 = 2915$ | $1.40 \times 10^{-3}$ |
| | $\upsilon_2 = 1534$ | $5.73 \times 10^{-1}$ |
| | $\upsilon_3 = 3019$ | $8.92 \times 10^{-4}$ |
| | $\upsilon_4 = 1306$ | 1.87 |
| $CO_2$ [19] | $\upsilon_1 = 1388$ | $4.73 \times 10^{-1}$ |
| | $\upsilon_2 = 677$ | 7.53 |
| | $\upsilon_3 = 2349$ | $1.34 \times 10^{-2}$ |

### 2.2. Acoustic spectra of single-relaxation processes

To describe the relation of multi-relaxation processes to single-relaxation processes, we first deduce the acoustic spectra of single-relaxation processes. For a gas with a single vibrational mode, the effective specific heat of the gas is [2, 21]

$$C_{\mathrm{V}}^{\mathrm{eff}}(\omega) = C_{\mathrm{V}}^{\infty} + \frac{C_{\mathrm{V}}^{\mathrm{vib}}}{1 + \mathrm{i}\omega\tau}, \tag{8}$$

where $\tau$ is the relaxation time characterizing the single-relaxation process [27, 28], $C_{\mathrm{V}}^{\infty}$ is the external specific heat from the translational and rotational degrees of freedom of molecules [29] and $C_{\mathrm{V}}^{\mathrm{vib}}$ is the vibrational specific heat, which is the internal specific heat $C_{\mathrm{V}}^{\mathrm{int}}$ of most molecules (except $H_2$) around room temperature [4].

$C_{\mathrm{V}}^{\infty}$ only depends on the molecular symmetry at room temperature: for diatomic and linear gaseous molecules, $C_{\mathrm{V}}^{\infty} = 5R/2$; for non-linear molecules, $C_{\mathrm{V}}^{\infty} = 3R$. $C_{\mathrm{V}}^{\mathrm{vib}}$ is calculated by the Planck–Einstein function [4]

$$C_{\mathrm{V}}^{\mathrm{vib}} = gR\left(\frac{\theta^{\mathrm{vib}}}{T_0}\right)\frac{\exp(\theta^{\mathrm{vib}}/T_0)}{(\exp(\theta^{\mathrm{vib}}/T_0) - 1)^2}, \quad \theta^{\mathrm{vib}} = \frac{h\upsilon}{k_{\mathrm{B}}}. \tag{9}$$

According to equation (9), $C_{\mathrm{V}}^{\mathrm{vib}}$ is determined directly by the characteristic frequency of vibrational mode $\upsilon$. Table 1 provides the vibrational frequencies expressed by the spectroscopic convention in terms of the inverse wavelength and the results of $C_{\mathrm{V}}^{\mathrm{vib}}$ for some gases at $T = 300\,\mathrm{K}$. Comparing $C_{\mathrm{V}}^{\mathrm{vib}}$ in table 1 with $C_{\mathrm{V}}^{\infty}$ of gases or mixtures ranging from 20.775 to 24.93 $\mathrm{J{\cdot}mol^{-1}\ K^{-1}}$, we can see $C_{\mathrm{V}}^{\infty} > C_{\mathrm{V}}^{\mathrm{vib}}$ and even $C_{\mathrm{V}}^{\infty} \gg C_{\mathrm{V}}^{\mathrm{vib}}$.

Using equation (8) and setting $C_{\mathrm{V}}^{\mathrm{eff}}(\omega) \equiv x(\omega) - \mathrm{i}y(\omega)$, the real and imaginary parts of $C_{\mathrm{V}}^{\mathrm{eff}}(\omega)$ for single-relaxation processes are

$$x_{\mathrm{s}}(\omega) = C_{\mathrm{V}}^{\infty} + \frac{C_{\mathrm{V}}^{\mathrm{vib}}}{1 + (\omega\tau)^2}, \quad y_{\mathrm{s}}(\omega) = C_{\mathrm{V}}^{\mathrm{vib}}\frac{\omega\tau}{1 + (\omega\tau)^2}. \tag{10}$$

Substituting (10) into $A_\mu$ in (7), it is evident that $A_\mu$ changes little with $\omega$ since $C_{\mathrm{V}}^{\infty} > C_{\mathrm{V}}^{\mathrm{vib}}$. Thus we can set $\omega\tau = 1$ in $A_\mu$ to obtain the general expression of acoustic spectra for single-relaxation processes:

$$\mu_{\mathrm{s}}(\omega) = A_{\mathrm{s}}C_{\mathrm{V}}^{\mathrm{vib}}\frac{\omega\tau}{1 + (\omega\tau)^2},$$
$$A_{\mathrm{s}} = \frac{\pi R}{C_{\mathrm{V}}^{\infty 2} + RC_{\mathrm{V}}^{\infty} + C_{\mathrm{V}}^{\infty}C_{\mathrm{V}}^{\mathrm{vib}} + RC_{\mathrm{V}}^{\mathrm{vib}}/2 + (C_{\mathrm{V}}^{\mathrm{vib}})^2/2}. \tag{11}$$

Equation (11) is deduced from the effective specific heat, and a thermodynamics approach confirms this equation [30]. In equation (11), $A_{\mathrm{s}}C_{\mathrm{V}}^{\mathrm{vib}}$ is independent of $\omega$ and determines the amplitude of $\mu_{\mathrm{s}}(\omega)$, while $\frac{\omega\tau}{1 + (\omega\tau)^2}$ is a bell-shaped function.

### 2.3. Acoustic spectra of multimode relaxation processes

Now we consider the acoustic spectra of multimode relaxation processes. For a gas mixture with $W$ kinds of molecules consisting of $N$ types of vibrational modes ($N \geqslant W$), the effective specific heat of the multi-relaxation process is the sum of interior single-relaxation processes [28, 31]:

$$C_{\mathrm{V}}^{\mathrm{eff}} = C_{\mathrm{V}}^{\infty} + \sum_{i=1}^{N}\frac{C_i^{\mathrm{int}}}{(1 + \mathrm{i}\omega\tau_i)}, \quad C_{\mathrm{V}}^{\infty} = \sum_{l=1}^{W}a_l C_l^{\infty}, \quad \sum_{l=1}^{W}a_l = 1, \tag{12}$$

where $C_l^{\infty}$ is the external specific heat of gas molecule $l$, $a_l$ is the mole fraction of molecule $l$ and $C_i^{\mathrm{int}}$ and $\tau_i$ are the internal specific heat and the relaxation time of the $i$th single-relaxation process, respectively. In [28], we proved that the number of decomposed single-relaxation processes equals the number $N$ of all vibrational modes of the component gas molecules. Using equation (12) and $C_{\mathrm{V}}^{\mathrm{eff}}(\omega) \equiv x(\omega) - \mathrm{i}y(\omega)$, the real and imaginary parts of $C_{\mathrm{V}}^{\mathrm{eff}}(\omega)$ for the multi-relaxation process are

$$x_{\mathrm{m}}(\omega) = C_{\mathrm{V}}^{\infty} + \sum_{i=1}^{N}\frac{C_i^{\mathrm{int}}}{1 + (\omega\tau_i)^2}, \quad y_{\mathrm{m}}(\omega) = \sum_{i=1}^{N}\frac{C_i^{\mathrm{int}}\omega\tau_i}{1 + (\omega\tau_i)^2}. \tag{13}$$

Since $C_{\mathrm{V}}^{\mathrm{int}} = \sum C_i^{\mathrm{int}} = \sum a_j C_j^{\mathrm{vib}}$ [28] and $C_{\mathrm{V}}^{\infty} > \sum a_j C_j^{\mathrm{vib}}$ (here $a_j$ is the mole fraction of vibrational mode $j$; all $a_j$ in the $l$th gas molecule are equal to $a_l$), so we have $C_{\mathrm{V}}^{\infty} > \sum C_i^{\mathrm{int}}$. Following the approach used to obtain equation (11), we substitute (13) into (7) and set all $\omega\tau_i = 1$ in $A_\mu$ to gain the general expression of acoustic spectra for multi-relaxation processes:

$$\mu_{\mathrm{m}}(\omega) = A_{\mathrm{m}}\sum_{i=1}^{N}C_i^{\mathrm{int}}\frac{\omega\tau_i}{1 + (\omega\tau_i)^2},$$
$$A_{\mathrm{m}} = \frac{\pi R}{C_{\mathrm{V}}^{\infty 2} + RC_{\mathrm{V}}^{\infty} + C_{\mathrm{V}}^{\infty}\sum C_i^{\mathrm{int}} + R\sum C_i^{\mathrm{int}}/2 + \left(\sum C_i^{\mathrm{int}}\right)^2/2}. \tag{14}$$

From equations (14) and (11), we can deduce the relationship between the acoustic spectra of multi-relaxation processes and those of single-relaxation processes.

### 2.4. Decomposition of acoustic spectra of multi-relaxation processes

According to equation (12), the internal specific heat of a multi-relaxation process can be regarded as the sum of all $\frac{C_i^{\mathrm{int}}}{1 + \mathrm{i}\omega\tau_i}$ of interior single-relaxation processes. Similar to

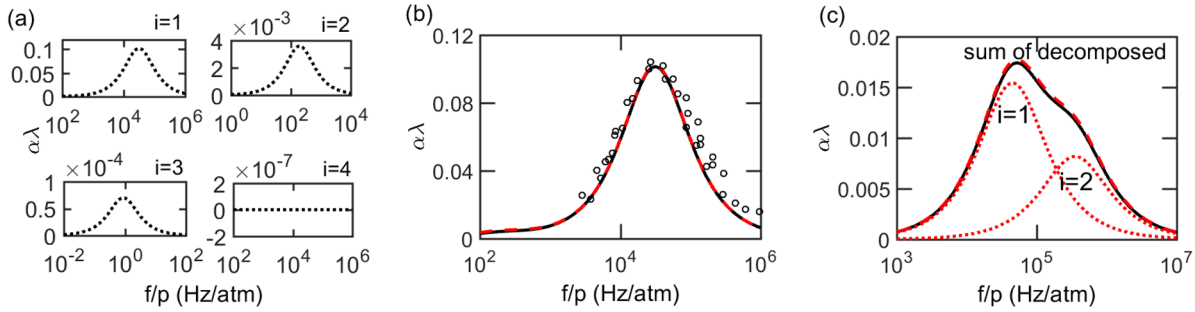


**Figure 1.** Decomposition of acoustic relaxation spectra of gases. (a) Decomposition of the spectrum of 80% $CO_2$–20% $N_2$ for all single-relaxation processes in equation (12). (b) Spectra and the sum of the decomposed spectra in (a) for 80% $CO_2$–20% $N_2$ (circles, experimental data [19]). (c) Spectra, decomposition and the sum of decomposed spectra of 40% $CH_4$–10% $Cl_2$–50% $N_2$ for the two dominant single-relaxation processes. The solid line represents the theoretical total multi-relaxation spectra; the dotted line is the decomposed single-relaxation spectra; and the dashed line is the sum of the decomposed spectra.

equation (8), we define the effective specific heats of these single-relaxation processes as

$$C_i^{\text{eff}} = C_{\text{V}}^{\infty} + \frac{C_i^{\text{int}}}{1 + \text{i}\omega\tau_i}, \tag{15}$$

and similar to equation (11), the acoustic spectra of these single-relaxation processes are obtained as

$$\mu_i(\omega) = A_i C_i^{\text{int}} \frac{\omega\tau_i}{1 + (\omega\tau_i)^2},$$

$$A_i = \frac{\pi R}{C_{\text{V}}^{\infty 2} + RC_{\text{V}}^{\infty} + C_{\text{V}}^{\infty} C_i^{\text{int}} + RC_i^{\text{int}}/2 + (C_i^{\text{int}})^2/2}. \tag{16}$$

Comparing (16) with (14), the only difference between $A_i$ and $A_{\text{m}}$ is $C_i^{\text{int}}$ and $\sum C_i^{\text{int}}$. Since $C_{\text{V}}^{\infty} > \sum C_i^{\text{int}}$, we have $A_i \cong A_{\text{m}}$. Therefore, the acoustic spectrum of a multi-relaxation process is essentially the sum of the spectra of interior single-relaxation processes:

$$\mu_{\text{m}}(\omega) = \sum_{i=1}^{N} \mu_i(\omega) = \sum_{i=1}^{N} A_i C_i^{\text{int}} \frac{\omega\tau_i}{1 + (\omega\tau_i)^2}. \tag{17}$$

In other words, we decompose the entire spectrum of a multi-relaxation process into $N$ spectra of single-relaxation processes.

One point should be noted in this decomposition. For $A_{\text{m}}$ in equation (14) and $A_i$ in equation (16) independent of the value of $\omega$ (from 0 to $\infty$), $A_i \cong A_{\text{m}}$, so equation (17) can be obtained. The reason we select $\omega\tau = 1$ is to make the peak values of the acoustic relaxation spectra more accurate.

### 2.5. Results of the decomposition

The binary gas mixture 80% $CO_2$–20% $N_2$ and the ternary mixture 40% $CH_4$–10% $Cl_2$–50% $N_2$ are used to illustrate the decomposition of acoustic relaxation spectra. According to equation (12), the number of decomposed single-relaxation processes equals the number of all vibrational modes of the component gas molecules [28]. Thus, the multi-relaxation spectra of $CO_2$–$N_2$ and $CH_4$–$Cl_2$–$N_2$ are decomposed into $N = 4$ and $N = 6$ spectra of interior single-relaxation processes, respectively.

As shown in figure 1(a), 20% $CO_2$–80% $N_2$ has only one significant decomposed single-relaxation spectrum ($i = 1$) which is almost equal to the multi-relaxation spectrum in figure 1(b) and three very small-amplitude decomposed spectra ($i = 2, 3, 4$) which can be ignored. For 20% $CO_2$–80% $N_2$, figure 1(b) shows that the sum curve (dashed) of decomposed single-relaxation spectra overlaps with the multi-relaxation spectrum (solid) by our general expression and matches the experimental data (circles) [19] very well.

Considering now the $N = 6$ single-relaxation processes for 40% $CH_4$–10% $Cl_2$–50% $N_2$, figure 1(c) shows only two dominant decomposed single-relaxation spectra (dotted) and the sum curve (dashed) of single-relaxation spectra overlaps with the multi-relaxation spectrum (solid) again. Therefore, our decomposition approach is confirmed and clearly illustrates the constructive characteristics of molecular multimode relaxation processes in gases.

According to the results of the decomposition, the multi-relaxation processes in gases are generally composed of one or two dominant single-relaxation processes. This explains why most multi-relaxation spectra generally have only one or two significant peaks in the relaxation (moderate) frequency range, as shown in figures 1(b) and (c). Based on this decomposition, we can reconstruct the entire molecular multi-relaxation process.

## 3. Reconstruction of molecular multimode relaxation processes

### 3.1. Method of reconstruction

According to equation (11), when $\omega\tau = 1$ (i.e. the acoustic period is commensurate with the relaxation time), the acoustic loss due to a molecular single-relaxation process is a maximum $A_{\text{s}} C_{\text{V}}^{\text{vib}}/2$. Thus the strength of molecular relaxation is manifested by the peaks of the relaxation spectra. So we define the peak amplitude $\varepsilon = AC_{\text{V}}^{\text{vib}}/2$ as the 'relaxation strength' corresponding to the relaxation time $\tau$. Thus equation (17) can be rewritten as

$$\mu_{\text{m}}(\omega) = \sum_{i=1}^{N} 2\varepsilon_i \frac{\omega\tau_i}{1 + (\omega\tau_i)^2}. \tag{18}$$

According to equation (18), $\varepsilon_i$ and $\tau_i$ define all interior single-relaxation processes in an entire multi-relaxation process.

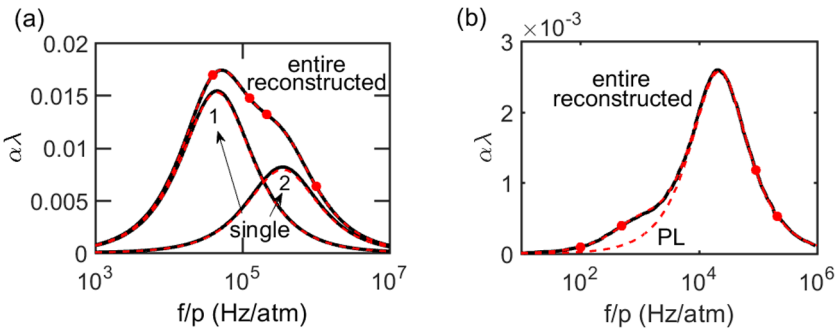


**Figure 2.** Reconstruction of the molecular relaxation processes of gases: (a) 40% $CH_4$–10% $Cl_2$–50% $N_2$, (b) 5% $CH_4$–95% $N_2$. Solid lines are the theoretical multi-relaxation spectra and decomposed single-relaxation spectra; bold dots are the spectral values at the measured frequency for the reconstruction; dashed lines are the reconstructed results of multi-relaxation spectra and decomposed single-relaxation spectra.

Therefore, the reconstruction of molecular relaxation processes captures $\varepsilon_i$ and $\tau_i$ from the measured acoustic absorption and sound speed.

In excitable gases, the acoustic absorption $\alpha$ is the sum of the relaxation contribution $\alpha_r$ and the classical contribution $\alpha_c$. $\alpha_r$ is related to the energy exchange between molecular internal and external degrees of freedom in the pairs of collisional molecules, while $\alpha_c$ is associated with transport phenomena, i.e. heat conduction, viscosity and diffusion. Since $\alpha_c$ is generally very small compared with $\alpha_r$ at the range of $f/p < 10^6$ Hz atm$^{-1}$, the classical contribution to the acoustic absorption can be omitted in the relaxation (moderate) frequency range without loss of generality [21]. In addition, the non-ideal behavior of gases is considered to be negligible in this work, and the correction [32–34] of our reconstructed results at high pressure and low temperature will be considered in future work.

With the measurements of acoustic absorption and sound speed at two frequencies, two spectral values, $\mu_s(\omega_1)$ and $\mu_s(\omega_2)$, can be calculated from equation (2). Using equation (11) and the two spectral values, we can capture the relaxation strength $\varepsilon$ and the relaxation time $\tau$ of a single-relaxation process as

$$\varepsilon = \frac{\mu_s(\omega_1)(1+(\omega_1\tau)^2)}{2\omega_1\tau},\quad \tau = \sqrt{\frac{\mu_s(\omega_2)\omega_1 - \mu_s(\omega_1)\omega_2}{\mu_s(\omega_1)\omega_2\omega_1^2 - \mu_s(\omega_2)\omega_1\omega_2^2}}. \tag{19}$$

Equation (19) is our previous two-frequency reconstruction algorithm for capturing the primary relaxation processes [22]. According to equation (18), the spectrum of the entire multi-relaxation process could have several peaks and cannot be replaced by a primary relaxation process completely. Solving $2N$ equations in the form of equation (18), which are evaluated with the values of $\mu_m(\omega)$ at $2N$ frequencies, we can obtain $\varepsilon_i$ and $\tau_i$ for $N$ decomposed single-relaxation processes and then reconstruct the entire molecular multi-relaxation process.

Obviously, equation (19) is the analytical solution of equation (18) when $N = 1$. Therefore, our previous two-frequency algorithm is a special case of the reconstruction method based on the decomposition approach described in this paper. In other words, our decomposition develops the reconstruction method from the primary (single) relaxation processes to the entire molecular multimode relaxation processes.

### 3.2. Results of reconstruction

Since gases and mixtures generally result from only one or two dominant single-relaxation processes [15–20], we now demonstrate how the method can use the measurements at four frequencies to reconstruct the entire molecular multi-relaxation process, based on equation (18) with $N = 2$.

Consider an acoustic sensing apparatus working at 40 kHz, 125 kHz, 215 kHz and 1 MHz to test the gas mixture 40% $CH_4$–10% $Cl_2$–50% $N_2$. The ambient conditions of this mixture are room temperature ($T = 293$ K) and standard atmospheric pressure ($P = 1$ atm). The measured sound speeds $c$ are 346.38, 347.22, 347.49 and 348.13 m s$^{-1}$ and acoustic absorption coefficients $\alpha_r$ are 1.9546, 5.3053, 8.1506 and 18.257 m$^{-1}$ at the respective operating frequencies (those values were calculated using our theoretical physical model [28, 35]). According to equation (2), the spectral values of $\mu(\omega)$ at the four selected frequencies are $1.6926 \times 10^{-2}$, $1.4737 \times 10^{-2}$, $1.3173 \times 10^{-2}$ and $6.3557 \times 10^{-3}$, respectively, shown as bold dots in figure 2(a). Using equation (18) and the four spectral values, the reconstructed results of two relaxation strengths and two relaxation times are $1.527 \times 10^{-2}$, $7.916 \times 10^{-3}$, $3.523 \times 10^{-6}$ s and $4.501 \times 10^{-7}$ s, respectively. The reconstructed results are reasonably close to the theoretical values of $1.542 \times 10^{-2}$, $8.169 \times 10^{-3}$, $3.511 \times 10^{-6}$ s and $4.497 \times 10^{-7}$ s, respectively. As shown in figure 2(a), the two reconstructed curves of decomposed single-relaxation spectra (dashed) overlap with the theoretical spectra (solid), as well as the reconstructed entire multi-relaxation spectrum. Therefore, our decomposition method is able to reconstruct the entire molecular multimode relaxation process.

For 5% $CH_4$–95% $N_2$, figure 2(b) shows the reconstructed primary relaxation spectrum (dashed) by the two-frequency algorithm of PL using at 92 and 215 kHz (the same as figure 3 in [21]) and the reconstructed entire relaxation spectrum (dashed) using our approach at 0.1, 0.7, 92 and 215 kHz. Compared with the entire theoretical curve (solid), our method reconstructs the entire relaxation process more effectively. The two-frequency algorithm misses the secondary relaxation process, having a peak to the left of the primary relaxation peak. Otherwise, the reconstructed spectrum of the primary relaxation process by PL is similar to our reconstructed spectrum of a single-relaxation process. Therefore,

**Table 2.** The relative errors of the relaxation strengths $\varepsilon_1$, $\varepsilon_2$ and the relaxation times $\tau_1$, $\tau_2$ of 40% $CH_4$–10% $Cl_2$–$N_2$ reconstructed from the measurements with ±5% errors at four selected frequencies.

| Frequencies:errors | The relative errors of $\varepsilon_1$, $\tau_1$, $\varepsilon_2$ and $\tau_2$ | | | |
|---|---|---|---|---|
| $f_1 = 40$ kHz: − 5% | −6.97% | −9.55% | −0.67% | −2.66% |
| $f_1 = 40$ kHz: + 5% | 1.25% | 4.36% | 2.34% | −0.8% |
| $f_2 = 125$ kHz: − 5% | −6.81% | 20.05% | 14.48% | 7.33% |
| $f_2 = 125$ kHz: + 5% | 3.12% | −16.53% | −13.04% | −12.14% |
| $f_3 = 215$ kHz: − 5% | 2.27% | −12.03% | −14.49% | −16.62% |
| $f_3 = 215$ kHz: + 5% | −8.20% | 12.77% | 18.22% | 12.98% |
| $f_4 = 1$ MHz: − 5% | −3.99% | −1.09% | 0.17% | 4.85% |
| $f_4 = 1$ MHz: + 5% | −2.35% | −4.06% | 2.17% | −7.22% |

our decomposition approach provides a method for capturing the molecular relaxation processes from single relaxation to multi-relaxation in gases.

### 3.3. Error analysis of the reconstruction

In the reconstruction procedures, the selected frequencies and the measurement spectral values both have determinative influences on the reconstructed results. Considering the measurement errors in these two aspects, the mixture 40% $CH_4$–10% $Cl_2$–$N_2$ is used in our simulations. The measured frequencies of 40 kHz, 125 kHz, 215 kHz and 1 MHz are labeled as $f_1, f_2, f_3$ and $f_4$, respectively.

Firstly, we fix the measured frequencies and observe the influence of the measurement errors of relaxation spectral values at each frequency on the reconstructed results. According to equation (2), the relaxation spectra are decided by the measurements of acoustic absorption and sound speed of the gases. Since the sound speed can be obtained accurately, we choose the acoustic absorption with relative errors of ±5% to reconstruct the entire multimode relaxation process. Table 2 shows the errors of the reconstructed relaxation strengths and relaxation times of the decomposed single-relaxation spectra.

From table 2, the measurement errors at $f_1$ mainly cause the errors in reconstructed decomposed single-relaxation spectrum 1 at low frequency, while the measurement errors at $f_4$ mainly cause the deviations of single-relaxation spectrum 2 at high frequency. Spectra 1 and 2 are labeled in figure 2. Since $f_2$ and $f_3$ are located in the ranges of both decomposed single-relaxation spectra 1 and 2, their measurement errors influence the reconstructions of spectra 1 and 2 and cause larger errors than $f_1$ and $f_4$.

According to the reconstructed results in figure 2, $f_1$ and $f_2$ should be located in the relaxation range of the decomposed single-relaxation spectrum 1 while $f_3$ and $f_4$ should be situated in the decomposed single-relaxation process 2. Thus, the selected $f_1$ is supposed to be less than the effective relaxation frequency of low-frequency decomposed spectrum 1 while $f_4$ is larger than the effective relaxation frequency of high-frequency decomposed spectrum 2. $f_2$ and $f_3$ should be evenly distributed between $f_1$ and $f_4$.

According to the simulations, when $f_1$ and $f_4$ cover the entire molecular multi-relaxation process, the frequency changes of $f_2$ and $f_3$ do not significantly influence the reconstructed errors resulting from their measurement errors. Once one of the decomposed single-relaxation processes is not covered by the range between $f_1$ and $f_4$, the single-relaxation spectrum would be missed in the reconstruction. Moreover, the values of $f_1$ and $f_4$ are difficult to determine for unknown gases. Thus, one needs to study the effects of different values of $f_1$ and $f_4$ on the reconstruction errors. Since the frequency changes of $f_1$ and $f_4$ would display similar simulation results, we choose $f_1$ with measurement errors to illustrate the effects.

In simulation, $f_1$ varies from the lower value of 10 kHz to the higher one of 50 kHz. Then we assume the error distribution of measured spectral values $\mu_1$ is uniform within ±10%, which is probably a worst case (the error distribution is more likely to have a Gaussian distribution). Figure 3 depicts the dependence of the errors of the reconstructed results, including the relaxation strengths $\varepsilon_1$, $\varepsilon_2$ and relaxation times $\tau_1$, $\tau_2$, on the selected frequencies and measured spectral values.

From figure 3, we can first see that the measurement errors at $f_1$ mainly cause the errors of $\varepsilon_1$ and $\tau_1$, as in table 2. The closer $f_1$ approaches to the effective relaxation frequency of the decomposed spectrum 1 (45 kHz), smaller errors in the reconstructed results and a more accurate spectrum can be obtained. It is also observed that the errors in the reconstructed relaxation results are approximately linear depending on the errors of the measured spectral values. The linear dependence reveals that the errors of the reconstructed results could be effectively reduced with averaging of multiple measurements. Thus, our proposed method could guarantee robust measurement results.

### 3.4. An application example from experimental data

To reconstruct the entire molecular multi-relaxation process in practice, we recommend that the range of working frequency covers all dominant single-relaxation processes of the tested gases. In other words, the frequency range should cover the peaks of the acoustic relaxation spectra. In order to capture all the dominant interior single-relaxation processes, four or more working frequencies should be distributed over the relaxation frequency range. Repeating measurements and averaging the reconstructed results is an effective and convenient approach to eliminate the deviations in reconstruction results.

The gas mixture 90% $CO_2$–10% $O_2$ at $T = 600$ K and $T = 450$ K [17] is used to illustrate the reconstruction from experimental data based on our recommendations. As shown

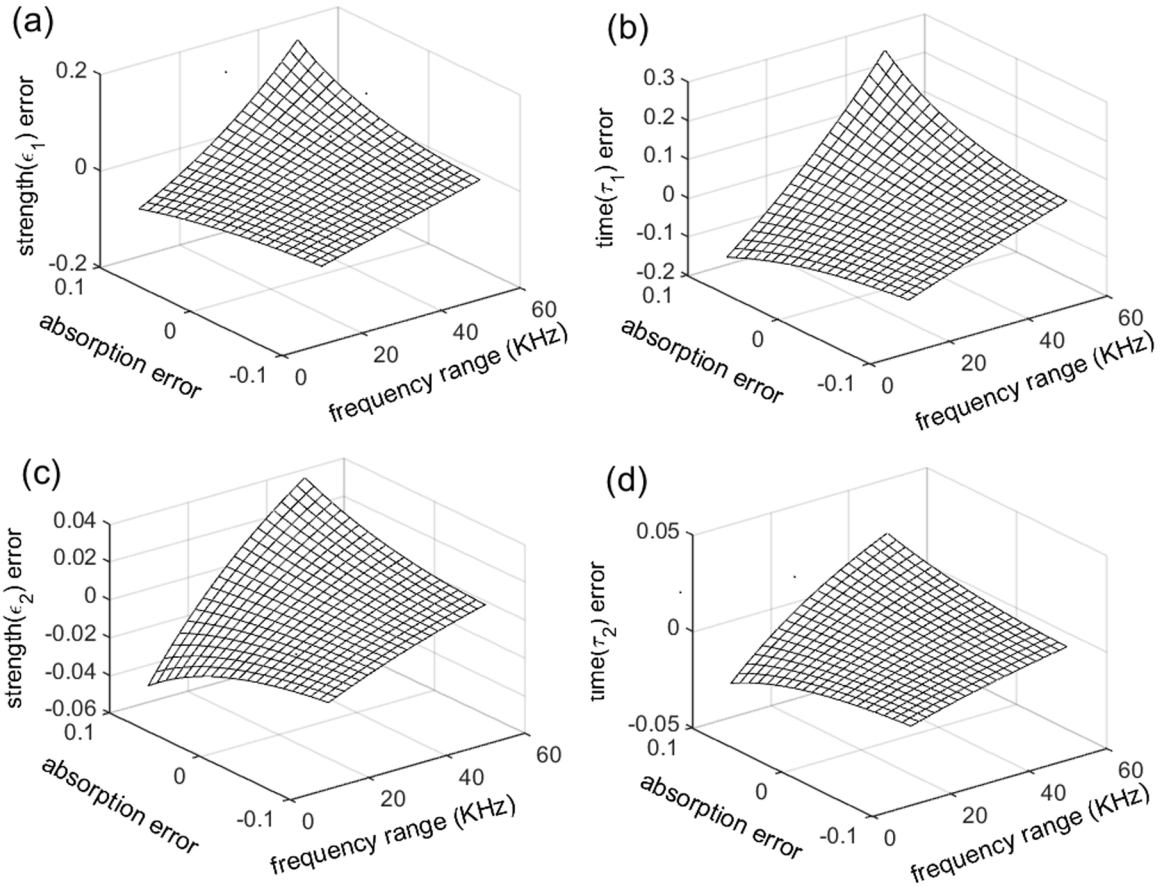


**Figure 3.** Dependence of the relative errors of reconstructed relaxation strengths $\varepsilon_1$ (a) and $\varepsilon_2$ (c) and relaxation times $\tau_1$ (b) and $\tau_2$ (d) on the measurement frequencies $f_1$ within 10–50 kHz and the relative errors of measured spectral values $\mu_1$ for the mixture of 40% $CH_4$–10% $Cl_2$–$N_2$ ($T = 293$ K, $P = 1$ atm).

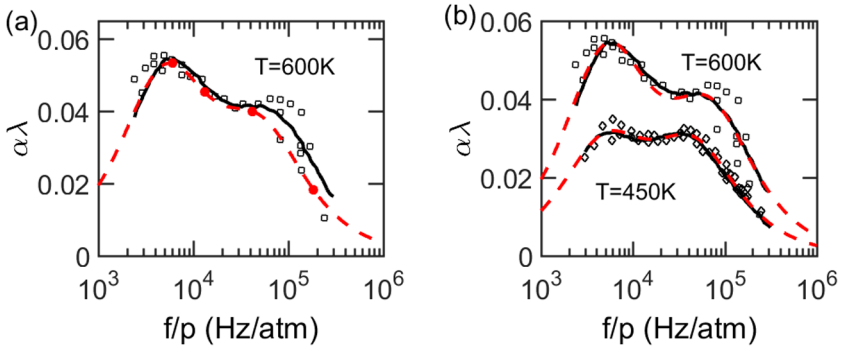


**Figure 4.** The capturing of acoustic relaxation from experimental data. Solid line, the theoretical multi-relaxation spectra; dashed line, the reconstructed multi-relaxation spectra from selected frequencies points (bold dots) with amplitude errors in (a) and the reconstructed acoustic spectra resulting from averaged relaxation strengths and relaxation times in (b); squares and diamonds, the experimental data for 10% $CO_2$–90% $O_2$ at $T = 600$ K and $T = 450$ K respectively [17].

in figure 4(a), we select the four experimental data points (bold dots) to reconstruct the entire molecular multi-relaxation process of 10% $CO_2$–90% $O_2$ at $T = 600$ K. The discrepancy between the reconstructed curve (dashed) and the theoretical spectrum (solid) [17] can primarily be attributed to the amplitude measurements of acoustic spectra of the analyzed gases, as shown in figure 4(a). In figure 4(a), the amplitudes of the four selected experimental data points deviate from the theoretical values of −2.20%, −4.24%, −3.15% and −27.38%. The reconstructed results of two relaxation strengths and two relaxation times are $2.97 \times 10^{-2}$, $4.74 \times 10^{-2}$, $3.00 \times 10^{-6}$ s and $3.20 \times 10^{-5}$ s, respectively. Compared with the theoretical relaxation strengths and relaxation times of $3.30 \times 10^{-2}$, $4.94 \times 10^{-2}$, $2.22 \times 10^{-6}$ s and $2.92 \times 10^{-5}$ s, the discrepancies of the reconstructed results are −10.0%, −4.05%, 35.1% and 9.59%, respectively.

Repeating measurements and averaging the reconstructed relaxation strengths and relaxation times is an effective approach to reduce the errors of reconstruction from experimental data. According to the recommended rule of working

frequency selection, we randomly select six groups of four experimental data points for 10% $CO_2$–90% $O_2$ at $T = 600$ K. The averaged results from the six captured groups of relaxation strengths and relaxation times are $3.31 \times 10^{-2}$, $4.95 \times 10^{-2}$, $2.25 \times 10^{-6}$ and $3.10 \times 10^{-5}$ s respectively, and the relative discrepancies to the theoretical values are only 0.3%, 0.2%, 1.4% and 6.2%.

As shown in figure 4(b), the two reconstructed acoustic spectra (dashed) by the averaged relaxation strengths and relaxation times nearly overlap with the theoretical spectra (solid) of 10% $CO_2$–90% $O_2$ at $T = 600$ K and $T = 450$ K. Therefore, the experimental data validate the reconstruction method based on the decomposition of entire molecular multi-relaxation processes in this paper. Given this case, our decomposition and reconstruction of molecular multi-relaxation spectra is robust when used within a wide temperature range.

## 4. Conclusion

In summary, we find that the frequency-dependent acoustic spectrum of a multi-relaxation process in gas is the sum of the spectra of decomposed single-relaxation processes. Based on this decomposition, we propose a method to capture the relaxation strengths and relaxation times of $N$ decomposed single-relaxation processes using sound speed and absorption measurements at $2N$ frequencies. This method can reconstruct the entire molecular multimode relaxation process in excitable gases. Compared with existing measurements and reconstruction algorithms, the reconstruction method based on the decomposition in this paper not only obtains the entire molecular multi-relaxation processes at a single pressure but avoids troublesome measurements of gas density. Therefore, the method provides a guide for an effective and simple design for instruments and sensors to measure molecular relaxation in gases, which would promote various applications.

## Acknowledgments

This work was supported by the National Natural Science Foundation of China (grant nos 61371139, 61571201 and 61461008) and the Natural Science Foundation of Hunan Province of China (grant no. 14JJ6046). We thank Professor Richard M Lueptow for helpful discussion.

## References

[1] Herzfeld K F and Rice F O 1928 Dispersion and absorption of high frequency sound waves *Phys. Rev.* **31** 691–5
[2] Herzfeld K F and Litovitz T A 1959 *Absorption and Dispersion of Ultrasonic Waves* (New York: Academic) p 59
[3] Lambert J D 1977 *Vibrational and Rotational Relaxation in Gases* (Oxford: Clarendon) p 48
[4] Dain Y and Lueptow R M 2001 Acoustic attenuation in three-component gas mixtures—theory *J. Acoust. Soc. Am.* **109** 1955–64
[5] Gordiets B F, Osipov A I, Stupochenko E V and Shelepin L A 1973 Vibrational relaxation in gases and molecular lasers *Sov. Phys. Usp.* **15** 759–85
[6] Grigorian G M and Kochetov I V 2008 Vibrational relaxation of highly excited CO molecules on $CO_2$ molecules in the active medium of a CO laser *Quantum Electron.* **38** 222–6
[7] Minami Y, Yogi T and Sakai K 2008 Thermal phonon resonance in nitrogen gas observed by Brillouin scattering *Phys. Rev.* A **78** 033822
[8] Tesch C M, Kurtz L and de Vivie-Riedle R 2001 Applying optimal control theory for elements of quantum computation in molecular systems *Chem. Phys. Lett.* **343** 633–41
[9] Tesch C M and de Vivie-Riedle R 2002 Quantum computation with vibrationally excited molecules *Phys. Rev. Lett.* **89** 157901
[10] Murphy D S, McKenna J, Calvert C R, Williams I D and McCann J F 2007 Ultrafast coherent control and quantum encoding of molecular vibrations in $D_2^+$ using intense laser pulses *New J. Phys.* **9** 260
[11] Jauberteau J L, Jauberteau I, Cinelli M J and Aubreton J 2002 Reactivity of methane in a nitrogen discharge afterglow *New J. Phys.* **4** 39
[12] Kozak T and Bogaerts A 2015 Evaluation of the energy efficiency of $CO_2$ conversion in microwave discharges using a reaction kinetics model *Plasma Sources Sci. Technol.* **24** 015024
[13] Chimenti D E 2014 Review of air-coupled ultrasonic materials characterization *Ultrasonics* **54** 1804–16
[14] McSweeney S G and Wright W M D 2012 A parallel-architecture parametric equalizer for air-coupled capacitive ultrasonic transducers *IEEE Trans. Ultrason. Ferroelectr. Freq. Control* **59** 90–7
[15] Shields F D 1960 Sound absorption in the halogen gases *J. Acoust. Soc. Am.* **32** 180–5
[16] Holmes R, Smith F A and Tempest W 1963 Vibrational relaxation in oxygen *Proc. Phys. Soc.* **81** 311–9
[17] Bass H E 1973 Vibrational relaxation *J. Chem. Phys.* **58** 4783–6
[18] Zuckerwar A J and Griffin W A 1980 Resonant tube for measurement of sound absorption in gases at low frequency/pressure ratios *J. Acoust. Soc. Am.* **68** 218–26
[19] Ejakov S G, Phillips S, Dain Y, Lueptow R M and Visser J H 2003 Acoustic attenuation in gas mixtures with nitrogen: experimental data and calculations *J. Acoust. Soc. Am.* **113** 1871–9
[20] Petculescu A, Hall B, Fraenzle R, Phillips S and Lueptow R M 2006 A prototype acoustic gas sensor based on attenuation *J. Acoust. Soc. Am.* **120** 1779–82
[21] Petculescu A G and Lueptow R M 2005 Synthesizing primary molecular relaxation processes in excitable gases using a two-frequency reconstructive algorithm *Phys. Rev. Lett.* **94** 238301
[22] Zhang K, Wang S, Zhu M and Ding Y 2013 Algorithm for capturing primary relaxation processes in excitable gases by two-frequency acoustic measurements *Meas. Sci. Technol.* **24** 055002
[23] Phillips S, Dain Y and Lueptow R M 2003 Theory for a gas composition sensor based on acoustic properties *Meas. Sci. Technol.* **14** 70–75
[24] Zhu M, Wang S, Wang S and Xia D 2008 An acoustic gas concentration measurement algorithm for carbon monoxide in mixtures based on molecular multi-relaxation model *Acta Phys. Sin.* **57** 5749–55 (http://wulixb.iphy.ac.cn/CN/Y2008/V57/I9/5749)
[25] Petculescu A and Lueptow R M 2012 Quantitative acoustic relaxational spectroscopy for real-time monitoring of natural gas: a perspective on its potential *Sens. Actuators* B **169** 121–7

[26] Hu Y, Wang S, Zhu M, Zhang K, Liu T and Xu D 2014 Acoustic absorption spectral peak location for gas detection *Sens. Actuators* B **203** 1–8
[27] Petculescu A G and Lueptow R M 2005 Fine-tuning molecular acoustic models: sensitivity of the predicted attenuation to the Lennard-Jones parameters *J. Acoust. Soc. Am.* **117** 175–84
[28] Zhang K, Wang S, Zhu M, Ding Y and Hu Y 2013 Decoupling multimode vibrational relaxations in multi-component gas mixtures: analysis of sound relaxational absorption spectra *Chin. Phys.* B **22** 014305
[29] Ben-Aryeh Y and Postan A 1974 Vibrational relaxation processes in a diatomic gas coupled to translational and radiational heat baths *Phys. Rev.* A **9** 2111–27
[30] Kneser H O 1965 *Relaxation Processes in Gases Physical Acoustics* vol II, ed W P Mason (New York: Academic) p 142
[31] Bass H E, Bauer H J and Evans L B 1972 Atmospheric absorption of sound: analytical expressions *J. Acoust. Soc. Am.* **52** 821–5
[32] Petculescu A and Achi P 2012 A model for the vertical sound speed and absorption profiles in Titan's atmosphere based on Cassini–Huygens data *J. Acoust. Soc. Am.* **131** 3671–9
[33] Hagermann A and Zarnecki J C 2006 Virial treatment of the speed of sound in cold, dense atmospheres and application to Titan *Mon. Not. R. Astron. Soc.* **368** 321–4
[34] Cramer O 1993 The variation of the specific heat ratio and the speed of sound in air with temperature, pressure, humidity, and $CO_2$ concentration *J. Acoust. Soc. Am.* **93** 2510–6
[35] Zhang K, Wang S, Zhu M, Hu Y and Jia Y 2012 Analytical model for acoustic multi-relaxation spectrum in gas mixtures *Acta Phys. Sin.* **61** 174301